



# Design, Experimental Tests, Modeling, and Optimization of a Particle Beam Width Probe (BWP) for the Aerodyne Aerosol Mass Spectrometer

J. ALEX HUFFMAN, Allison C. Aiken, and Jose-Luis Jimenez, Dept. of Chem. and CIRES, Univ. of Colorado at Boulder  
John T. Jayne, Timothy Onasch, and Doug R. Worsnop, Aerodyne Research Inc., MA  
Frank Drewnick, Max Planck Institute for Chemistry, Mainz, Germany



## INTRODUCTION

The Aerodyne Aerosol Mass Spectrometer (AMS) can provide real-time information on mass concentrations of chemical species in/on submicron aerosols, as well as on chemically-resolved size distributions. It uses an aerodynamic lens to focus the particles into a narrow beam, which is directed to the AMS detector. The particle-focusing characteristics of the aerodynamic lenses are dependent on the size and physical shape of the particles. The measurement of particle beam width is of interest for two reasons: (1) it provides a real-time surrogate non-sphericity measurement and (2) provides verification that all particles impact the vaporizer, and allows for correction if this is not the case. For these reasons, a beam width probe (BWP) was designed and implemented for the Aerodyne Aerosol Mass Spectrometer (AMS), although this approach is also applicable to other instruments that use aerodynamic lens inlets. A computer model was developed to optimize the BWP and aid in the understanding of particle beams.

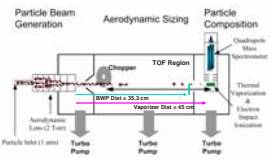


Fig. 1: AMS Schematic Diagram (with dimensions of 45 cm chamber)

## 1. Definition of Non-Sphericity Index

Since spherical particles have the smallest beam widths and non-spherical particles have broader beams, we can define a surrogate non-sphericity parameter,  $\nu$ , that we will call the lift shape factor, as:

$$\nu = \frac{\sigma_{z,app}}{\sigma_{z,sph}}$$

Where  $\sigma_{z,app}$  is the beam width for a sphere of a given vacuum aerodynamic diameter, and  $\sigma_z$  is the beam width for the particle of interest at the same  $d_{v,aer}$ . Only non-spherical particles experience lift forces<sup>5</sup> while for spherical particles lift forces are zero. Given the ease with which the measurement of  $\nu$  can be performed with the BWP described here and the larger difficulty of determining the dynamic shape factor ( $\chi$ ), future research should explore the relationship between these two.

## 2. Def'n of Particle CE due to Shape

To characterize the effect of shape on particle focusing, we define here the AMS collection efficiency due to irregular shape, and as a function of particle size as  $CE_i(d_{p,i})$ . This is the percentage of particles physically hitting the vaporizer, relative to spheres of the same vacuum aerodynamic diameter ( $d_{v,i}$ ). The current understanding of particle detection in the AMS indicates that low-volatility solid particles such as dry  $(NH_4)_2SO_4$  can also be lost due to bounce off the vaporizer surface ( $CE_b$ ). Note that in the absence of other physical effects that lead to particle loss,  $CE = CE_i * CE_b$ . These affects are

## BEAM WIDTH PROBE SET-UP AND JUSTIFICATION

summarized in a light blue box to the lower right.

### 3. Particle Beam Model

The particle beam is close to a point source at the exit of the lens (~100  $\mu$ m diameter)<sup>2</sup>. We assume that as the particles travel in the vacuum chamber the lateral spread of the particle beam in the direction perpendicular to its travel ("beam width") increases linearly with the distance traveled. Alternatively, the size of a particle beam can be related by the solid angle it fills. A cone having base area  $A$  and height  $h$  will define a solid angle approximated by  $W = A/h^2$ . We will assume that the particle density in the beam can be represented by a 2-D Gaussian distribution (Figure 2) as given by the following:

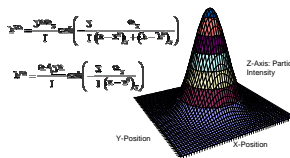


Fig. 2: 2-D Gaussian Distribution

The integrated volume under the Gaussian curve is shown in Figure 3a (for all angles,  $\theta$ ), indicating the probability density of particle impact. The area under each curve is conserved. Figure 3b is an integration of the first, showing the region of 100% collection shifts out for larger values of  $\sigma$ .

### 4. Beam Width Probe Design

A beam width probe was designed and implemented to provide a real-time quantitative measurement of the particle beam. Figure 4 shows a schematic of the probe set-up from the front and side. When the probe is in a blocking position, some incoming particles do not reach the vaporizer, and the AMS signal is reduced proportional to their mass. By moving the probe across the particle beam, the beam attenuation can be mapped, as shown in Figure 5.

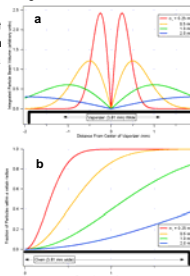


Fig. 3: Probability Distribution

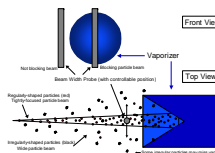


Fig. 4: Beam Width Probe (BWP)

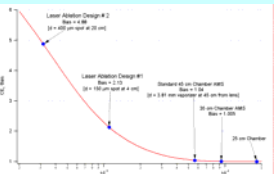
## CONCLUSIONS

- Aerodynamic lenses focus particles into narrow beams, that diverge upon leaving the lens as a function of particle size and shape.
- Measuring the particle beam width provides: (1) a real-time surrogate measure of particle non-sphericity (here we define  $\nu$ , the lift shape factor), and (2) an estimation of possible losses due to shape effects ( $CE_i$ )
- Beam width values were determined for laboratory-generated particles. Very well-focused particles exhibit a  $\sigma_z$  of 0.25 mm, with a corresponding  $CE_i$  of 1.0, whereas soot particles<sup>3,4</sup> are poorly focused and exhibit  $\sigma_z$  of 0.77 mm, with  $CE_i$  of 0.96.
- An optimal wire probe diameter of approximately 1.0 mm provides optimal sensitivity to both  $\sigma_z$  and  $CE_i$  for a range of realistic ambient particle types.
- A comparison of estimated bias against very irregular particles between the AMS and two other particle MS designs has been shown. The AMS shows a bias of 1.04, while the two other instruments show values of 2.13 and 4.88 respectively. Reducing AMS chamber length by 10 cm decreases the bias to 1.005.

## ACKNOWLEDGMENTS

The authors thank Ann Middlebrook of NOAA, Alicia Dellis of the Univ. of Colorado, and James Allan of UMIST for helpful discussions. We also thank EPA SPIR (grant EP-D04-008), NASA Earth System Science (grant NNG04GA673), and NASA ESS Graduate Fellowship (grant NGT5-30516) for funding.

## Relative Bias Comparison



The figure to the above shows a comparison of the relative detection bias between spherical, "well-focused" ( $\sigma_z = 0.25$  mm) and "poorly-focused" ( $\sigma_z = 0.77$  mm) soot particles for three common particle MS designs. Beams comprised of perfectly spherical particles are most easily detected by all instruments, because of the very narrow distribution of particle radial locations. Because the laser spot size in each laser-ablation instrument is small, however, the percentage of particles collected from a wide beam is therefore also small and the detection is more sensitive to the particle beam width.<sup>4,5</sup> The AMS has an advantage, because of the relatively large solid angle of collection, due to its large vaporization surface as compared to typical laser spot sizes.

## REFERENCES

- Liu, P., P.J. Ziemann, D.B. Kittelson, and P.H. McMurry. Generating Particle Beams of Controlled Dimensions and Divergence. 1. Theory of Particle Motion in Aerodynamic Lenses and Nozzle Expansions. *Aerosol Science and Technology*, 22 (3), 293-313, 1995.
- Heberlein, J., O. Postel, S. Girshick, P. McMurry, W. Gerberich, D. Iordanoglou, F. Di Fonzo, D. Neumann, A. Gidwani, M. Fan, and N. Tsimak. Thermal plasma deposition of nanophasse hard coatings. *Surface & Coatings Technology*, 142, 265-271, 2001.
- Slawik, J.G., K. Strömken, P. Davidovits, L.R. Williams, J. Jayne, C.E. Kolb, D. Worsnop, Y. Rudich, P. DeCarlo, and J. Jimenez. Particle Morphology and Density Characterization by Combined Mobility and Aerodynamic Diameter Measurements. Part 2: Application to Combustion Generated Soot Particles as a Function of Fuel Equivalence Ratio. *Aerosol Science and Technology*, Submitted 2004.
- Slawik, J.G. Poster 4P83

## 5. BWP Model Results and Verification

Figures 5a and 5b show the modeled transmission curves for probe diameters of 0.55 mm and 1.51 mm, which are optimal for narrow and wide beams respectively (see section 6). Each curve shows the percentage beam transmission (normalized to an unattenuated beam) as the probe is moved across the front of the vaporizer. For an extremely narrow beam ( $\sigma_z = 0.01$  mm), particle beam attenuation is only predicted within the wire shadow cast onto the vaporizer.

Before using the model to optimize BWP, we performed laboratory experiments to test the assumption that the particle beam can be approximated by a 2-D Gaussian

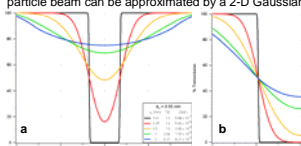


Fig. 5: Modeled Transmission Curves

distribution. Figure 6 shows results for three pure species (polydisperse). Least square fits were used to determine the best fit beam width ( $\sigma_z$ , where the subscript s refers the standard AMS chamber length of 45 cm from lens exit to vaporizer). Oleic acid particles, which are known to be spherical,

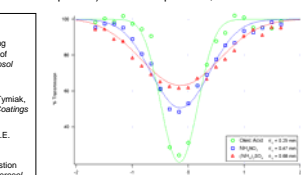


Fig. 6: Laboratory BWP Data

## MODEL DESCRIPTION AND RESULTS

$$S_{\sigma} = \frac{da}{d\sigma} \quad S_{CE_i} = \frac{dCE_i}{dCE_i}$$

where  $a_0$  is the attenuation at the center. Figure 8 shows the difference between curves similar to Figure 5. Regions of maximum difference between curves represents high sensitivity. Figure 9 also summarizes BWP sensitivity. Figure 9a shows  $da/d\sigma_z$ ,  $d\sigma_z/dCE_i$ , and  $da/dCE_i$  curves for the 0.5 mm wire. Figure 9b shows  $da/d\sigma_z$  plotted for a series of wires, and  $\sigma_z$  values, in order to determine the optimal wire for every beam width. Figure 9c shows the same analysis for  $CE_i$ .

### 7. Collection Efficiency due to Shape

Figure 7 also shows that an AMS chamber decreased in length by 10 cm will result in an increased  $CE_i$  for soot particles (considered to be the limit of a wide beam) to over 0.99.

### 6. BWP Optimization

By running the model for a variety of probe (wire) diameters ( $d_p$ ), we can determine an optimal wire probe with maximum sensitivity to measure  $CE_i$  or  $\nu$ . Sensitivity with respect to beam width,  $S_{\sigma}$  or  $CE_i$ ,  $S_{\sigma}$  are defined as:

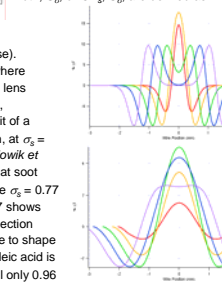


Fig. 7: Collection Efficiency due to Shape

This information can be summarized also by Figure 10. This plot can be helpful by determining  $\sigma_z$  values quickly, as a function only of transmission values at the wire positions used in the study.

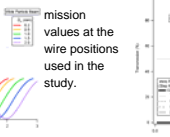


Fig. 8: Transmission Difference Curves

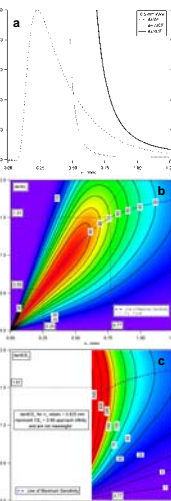
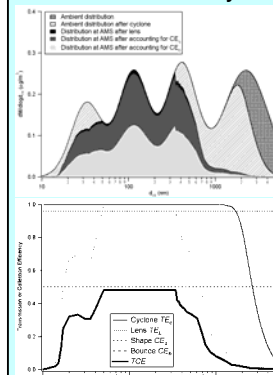


Fig. 9: Sensitivity Plots

Fig. 10: Transmission vs. Sigma (with laboratory data)

## AMS CE Summary



A hypothetical mass distribution with four modes was used to show the particle loss affects of within the AMS-sampling system. Note that it would be unlikely to observe such a complex distribution in ambient data. The top plot shows particle loss due to various physical effects, while the bottom plot shows just those effects. These include effects due to  $PM_{2.5}$  size cut, lens transmission, shape, and particle bounce, with the light gray region indicating the signal portion of the distribution detectable by the AMS.

- Cizzio, D., P. DeMott, C. Brock, P. Hudson, B. Jesse, S. Kreidenweis, A. Prenni, J. Schreiner, D. Thomson, and D. Murphy. A Method for Single Particle Mass Spectrometry of Ice Nuclei. *Aerosol Science and Technology*, 37, 460-470, 2003.
- Gard, E., Mayer, J.E., Morral, B.D., Davies, T., Ferguson, D.P., and Prather, K. A real-time analysis of individual atmospheric aerosol particles: design and performance of a portable ATOFMS. *Analytical Chemistry* 69: 4083, 1997.